Final Report
August 1988

To: National Aeronautics and Space Administration
Goddard Space Flight Center
Greenbelt, MD 20771

Contract: NAS5-28758

Title: Spectral characteristics and the extent of paleosols of the Palouse formation

Principal Investigator: Dr. B. E. Frazier
Agronomy and Soils
Washington State University
Pullman, WA 99164

Collaborators: Dr. Alan Busacca

Yaan Cheng
Agronomy and Soils

David Wherry

Judy Hart

Steve Gill
Digital Image Analysis Laboratory

INTRODUCTION:

In this document, results are reported by objective as stated in the original proposal. Objectives are reprinted here for clarity and they dictate the organization of this report.

RESULTS BY OBJECTIVE:

I. Test the hypothesis that TM data is adequate in band selection and width and in spatial resolution to distinguish soil organic matter, iron oxide and lime-silica contents to map several severity classes of erosion in soils of the Palouse region.

   A. Develop spectral relationships from TM data that will define the spatial distribution of soil areas by levels of (1) organic matter in the surface soil, (2) iron oxide and clay in exposed paleosol B horizons, and (3) lime-silica accumulations in exposed paleosol B horizons.

   B. Compare areas determined by the method outlined in A to patterns interpreted from color aerial photographs, and to ground observations on bare-soil fields.

   C. Define, on the basis of results of A and B to the extent possible, where exposed paleosols exist within fields that are not bare, but have a crop cover, and the distribution of desirable and undesirable soil properties in each field.

SUPPORTING LITERATURE

Upon investigation of the literature about spectral relationships, we found that other scientists have used band ratios, partly to reduce the effects of environmental factors which affect all bands equally, and partly to show unique information not seen with single band data (Jensen, 1986). The advantages of using band ratios were demonstrated by Kriegler et al. (1969). They found that ratios tend not to change when spectral signals change because of multiplicative factors, e.g., illumination factors like shadows and time of day or reflectance factors like scan angle, sun angle, species, maturity of plants and vigor. They also point out that these relationships are not perfect and will be less reliable when the two wavelengths being ratioed are widely separated. Kauth et al. (1979) pointed out that the band 7 to 5 ratio from Landsat multispectral scanner (MSS) data was very insensitive to changes in direct illumination on a scene. Kanemasu (1974) showed that this was true for a crop canopy as well using the 545/655 nm ratio. The ratio changed with crop development, but not with illumination angle. For these reasons, we chose to place most of our emphasis on using band ratios to achieve our objectives.

METHODS and SITE DESCRIPTION

This study used TM data collected 17 July, 1985 (scene 50503 18070 at WRS 43-27) and 14 July, 1984 (scene 50135 18054 at WRS 43-27). The

data were received from NASA via Earth Observation Satellite Co. (EOSAT) as fully processed computer compatible tapes (CCT-PT) and were corrected to the UTM coordinate system. No other corrections were made. Image data were analyzed using the VICAR/IBIS software system (Hart and Wherry, eds., 1984) and the Digital Image Analysis Laboratory (DIAL) at Washington State University.

Image processing consisted of several iterations of clustering, plotting clusters and mapping clusters derived from three bands of ratioed data. Ratios were chosen from bands having dissimilar reflectance patterns for known areas. Selected ratios were TM 1/4, 3/4, 5/4 and 5/3. Clustering was done on test areas which included a variety of bare soils and cropped soils. Clusters were plotted in two dimensions using the mean digital number (DN). The cluster plots were studied to detect predictable patterns which would yield information about the site. They were also mapped so that they could be correlated to information derived from ground sampling. The test fields and areas surrounding the test fields were then classified using a maximum likelihood algorithm (VICAR program BAYES) or a combination of parallelepiped and maximum likeihood techniques (VICAR program FASTCLAS). Classified areas were then field checked.

Ground data were collected near the time of overpass by transecting several test fields, writing soil descriptions and taking surface samples for analysis. The fields were sampled again later according to patterns developed by image analysis. Soil samples were collected from 3 X 3 pixel squares within each mapped area. Organic carbon, carbonate content, and iron oxides analyses were conducted on 76 selected samples. Organic carbon was determined by the modified Schollenberger (1927) procedure of Nelson and Sommers (1975), free iron oxides by the citrate-bicarbonate-dithionite procedure of Kittrick and Hope (1963), amorphous iron by the hydroxylamine method of Ross et al. (1985), and calcium carbonate content by the electronic manometer method of USDA (1984).

The Palouse is an ideal outdoor laboratory in which to study composite spectra of soils and plants (Figure 1). The summer dry season leaves the soils with little moisture variation at the surface by mid-July. Many fields are in rotations which include summer fallow. During the summer fallow part of the rotation, fields are harrowed several times and maintained weed-free throughout the summer, providing a smooth surface, also with little dry crop residue; an ample opportunity to collect good bare soil data. Summer fallow fields that had not been harrowed immediately before the date of imagery supply examples of partially covered soil by weed plants. Still other fields have complete cover by crop plants, some green and some ripened.

All of the soils in our study area are developed in loess parent material so all contain similar sized particles and have a silt loam or silty clay loam texture. The soils have incurred various amounts of erosion from none in the low areas to complete removal on some convex ridges. Where severe erosion has occurred, there is complete exposure of ancient soil B horizons (called paleosols). These are characterized

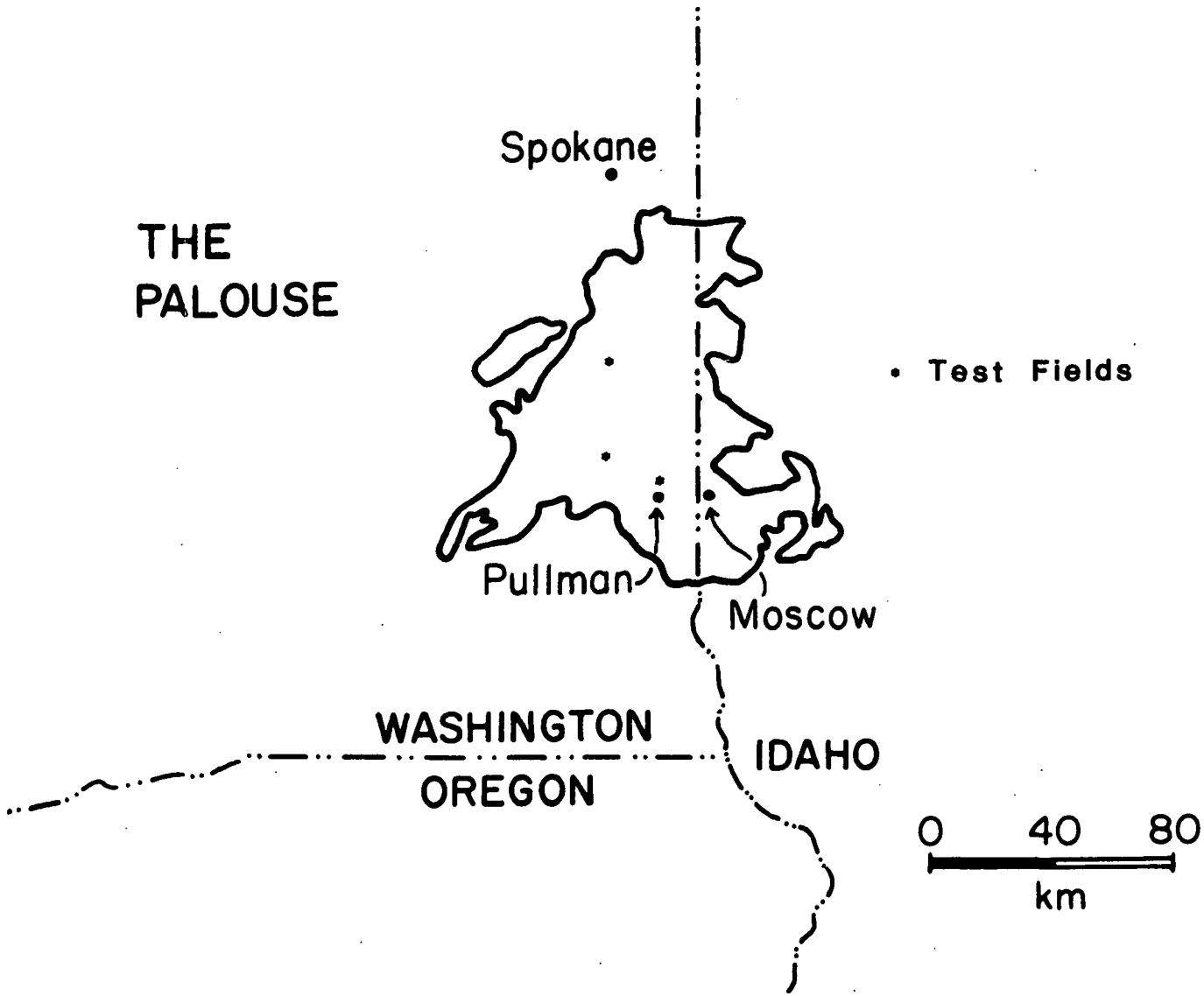

Figure 1. The main body of the Palouse formation showing the location of test fields used in this study.

as having accumulations of either secondary carbonates, clays or iron oxides and are called Bk, Bt or Bw horizons, respectively. No attempt was made to separate the Bw and Bt horizons spectrally. They are referred to collectively as Bw/Bt horizons. The entire landscape is underlain with these old soils representing previous cycles of soil formation and erosion. Over the span of geologic time known as the pleistocene the Palouse region was constructed from cycles of loess deposition, soil formation, and erosion by rainfall and snowmelt runoff. This process has created a landscape which is gently rolling, but with significant hills with slopes approaching 50% in some places (Frazier and Busacca, 1987).

The Palouse region has a Mediterranean climate, with dry summers, and receives 400 to 500 mm of precipitation as rain and snow during the winter. This is only enough water to provide stress-free plant growth on broad summits of hills, north-facing slopes and in low areas. Thus there is variation in the amount of organic matter production and storage in the soils and there is variation in reflectance of light from the soils.

SIGNIFICANT FINDINGS

Site One

The soil distribution pattern over the first site that we investigated included a mixture of exposed paleosols with Bk, Bw, and Bt horizons at the surface, and the usual A horizons. This provided a surface with a range of organic matter, lime-silica, iron and clay contents.

Plots of cluster analysis outputs revealed distinct groupings of reflectance data representing green crops, ripened crops, soil and green plants, and bare soil. A unique triangular shaped distribution was formed when TM 5/4 was plotted against 3/4 (Figure 2). Clusters of data from green crops tended to form a point near the origin of the plot and bare soil clusters formed the opposite side of the triangle. Ripened crops were found near the middle and lower edge, making a bulge in the lower side of the triangle. This relationship appears to be similar to the "peak of greenness" and the "plane of soils" concept of the Tasseled Cap transformation (Crist and Cicone, 1984; Kauth and Thomas, 1976). In this case, the distribution is created by the combined reflectance features of plants and soils. Without plants, only the soil line clusters would be shown. As the density of plants increases so does the reflectance in TM 4, and at the same time the reflectance in TM 3 and TM 5 decrease. In TM 3 the energy is absorbed by chlorophyl and in TM 5 it is absorbed by water in the plant leaves and/or is decreased by shadows caused by plant leaves. Thus the ratios 5/4 and 3/4 both tend to decline as plant cover increases, ultimately reaching a point near the origin of the plot and forming a triangle with the soil line as one side.

It was noted that all bare soil areas were represented by clusters forming the soil line located opposite the lower left point of the

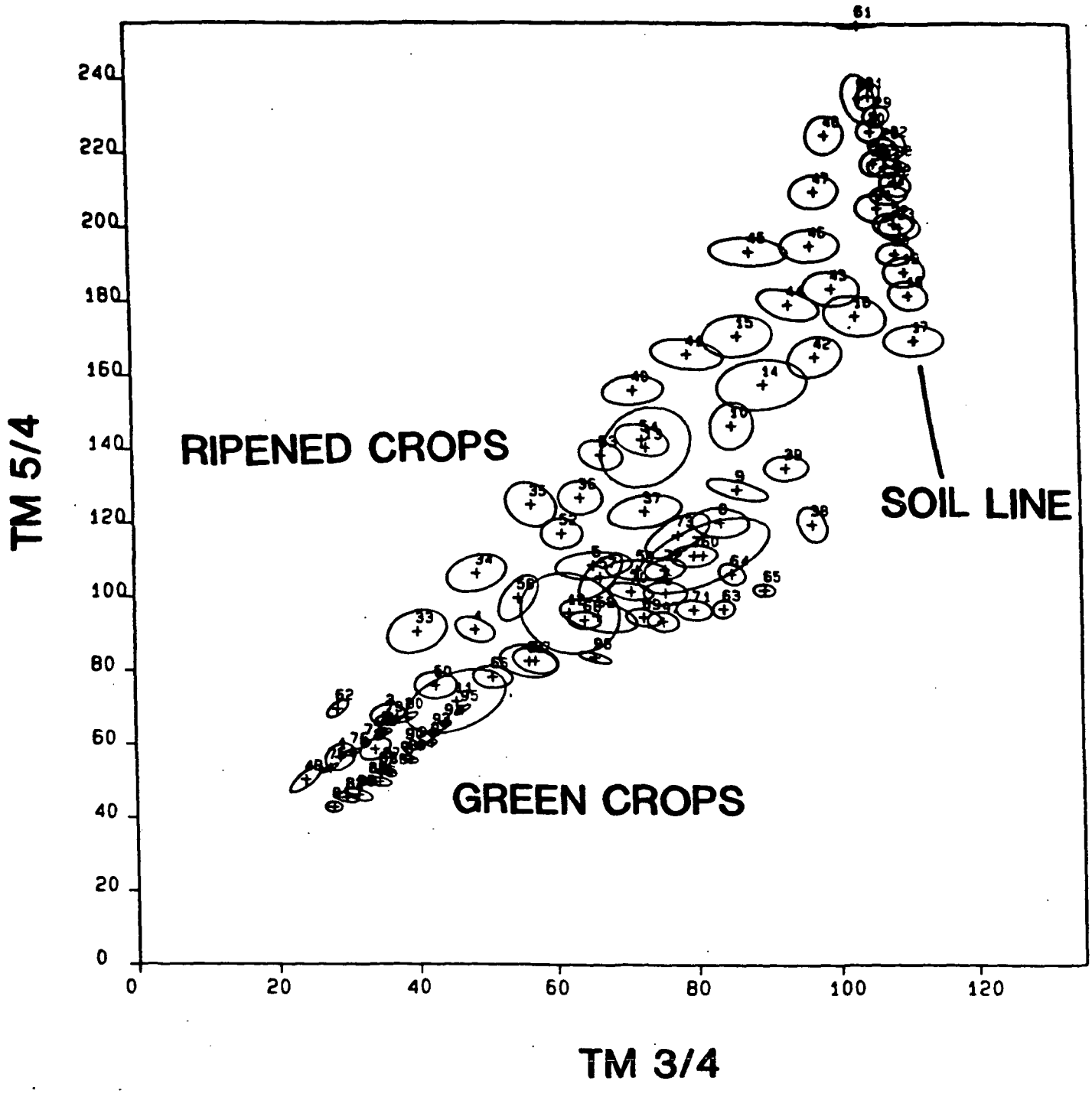

Figure 2. Cluster distribution of TM ratios 1/4, 3/4, 5/4, viewed from the 3/4 side. The soil line and point of greenness are displayed from this viewpoint.

triangle. When these clusters were mapped, a pattern of soil brightness emerged; clusters at the low end of the line represented light colored soils and clusters at the high end, dark colored soils. It was not possible however, to see the distribution of clusters in the middle of the line until the clusters were plotted using TM 5/4 and 1/4 (in effect, rotating the plot about the y-axis). When rotated, the soil line appeared as a plane and a line of clusters from areas containing water emerged (Figure 3).

By trial and error mapping of the clusters in the soil plane it was possible to group them into logical classes which fit various portions of the landscape. Clusters representing light colored soils mapped out on eroded knobs and dark colored soils appeared appropriately in low topographic positions and on north-facing slopes. In this fashion, all clusters in the soil plane shown in Figure 3 were placed into categories of landscape position. Clusters 17 and 18 represented eroded knobs and, proceeding to the upper right corner of the diagram, the next groups were from steep south-facing slopes, moderate south slopes, summits and north slopes, and flat low-lying areas.

Surface soil samples were taken from verifiable positions within each mapped group of clusters. The one soil characteristic which allowed separation of these clusters, or groups of clusters, was organic carbon. This is shown in Table 1 by landscape position of the clusters. Clusters 17 and 18 are shown separately as exposed Bk and Bw/Bt horizons which represent extremely eroded sites. No clusters were found which would allow separation of Bw and Bt horizons. Statistical tests were used to determine whether the groups of clusters, which were derived empirically and which looked separable on maps and aerial photographs, were numerically separable. Since the standard deviations of the carbon values increased as the means increased, the statistical analysis was done on log transformations of the means.

The LSD test showed correctly that the extremely eroded sites (Bk and Bw/Bt) were not different with respect to organic carbon content and should appear as one group of clusters (but not necessarily as one cluster because they were different with respect to their contents of carbonates and iron). The other groups were separable, indicating that the chosen boundaries matched well with the landscape positions. The groups showed different amounts of organic carbon resulting from differences in plant growth conditions on the various landscape positions. The difference in organic carbon values between the closest groups was 0.4%. This was perceived as a very good level of separation, one which should be useful to analyses of agricultural soils, particularly since phosphorus fertility is strongly correlated to organic carbon (personal communication, D. J. Mulla, 1987).

The relationships of the soil line were also investigated using regression analyses. The means of DN values of the ratio bands for each of the landscape classes were regressed against the means for organic carbon within each landscape class. Results showed that the soil line was affected strongly by organic carbon (Table 2). Based on

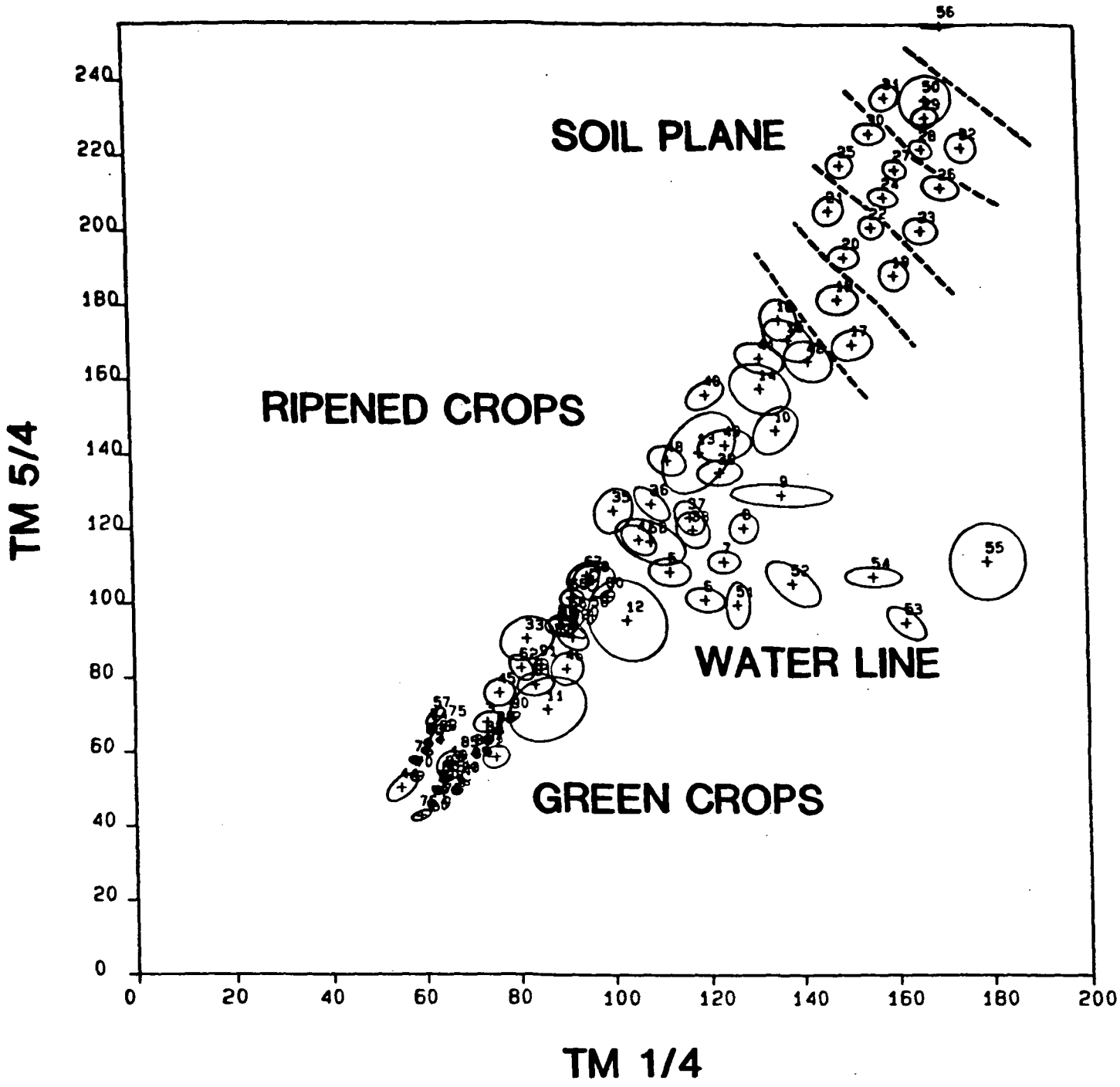

Figure 3. Cluster distribution of TM ratios 1/4, 3/4, 5/4, viewed from the 1/4 side. The soil line is shown as a plane.

Table 1. T tests (LSD) for carbon value.

	Carbon	Transformed Mean	
	%		
Bk Paleosols	0.43	-0.9022	A
Bw/Bt Paleosols	0.53	-0.6620	A
Steep South Slopes	1.00	-0.0174	B
Moderate South Slopes	1.38	0.2853	C
Summits and North Slopes	1.78	0.5666	D
Flat, Low-Lying	2.54	0.9329	E

Alpha = 0.05 DF = 67 MSE = 0.50
Critical value of T = 1.996
Least Significant Difference = 0.266
Means with the same letter are not significantly different

Table 2. Regression analysis of organic carbon and average DN value of TM band ratios.

Regression Output:TM1/TM4			Organic Carbon	Estimated Org. C
Constant		-11.8656		
Std Err of Y Est		0.195542	0.48	0.54
R Squared		0.952995	1.00	0.87
No. of Observations		5	1.45	1.45
Degrees of Freedom		3	1.78	2.03
			2.54	2.36
X Coefficient(s)	0.082705			
Std Err of Coef.	0.010604			

Regression Output:TM3/TM4				
Constant		30.10176		
Std Err of Y Est		0.125760	0.48	0.39
R Squared		0.980557	1.00	1.18
No. of Observations		5	1.45	1.45
Degrees of Freedom		3	1.78	1.72
			2.54	2.51
X Coefficient(s)	-0.26529			
Std Err of Coef.	0.021567			

Regression Output:TM5/TM4				
Constant		- 4.08519		
Std Err of Y Est		0.041529	0.48	0.47
R Squared		0.997879	1.00	1.01
No. of Observations		5	1.45	1.42
Degrees of Freedom		3	1.78	1.84
			2.54	2.51
X Coefficient(s)	0.025865			
Std Err of Coef.	0.000688			

this analysis any of the ratio bands could be used to model organic carbon content of bare soil, but the best single ratio was 5/4. The resultant model for organic carbon (%) as a function of TM 5/4 is illustrate Figure 4. Error bars are standard error of carbon values for each observation of mean DN. The equation is $Y = -4.08 + 0.026(TM\ 5/4 * 100)$, $R^2 = 0.99$.

Site Two

At a second site we tested four models which dealt with these objectives, the carbon model developed at the first site and three new models for iron and combinations of iron with carbon. Soils at the second site were different in that Bk horizons were absent and more of the area had Bw/Bt horizons exposed. The models used TM band ratios of 1/4-5/2-3/1 for organic carbon, 5/3-3/1-4/5 for amorphous iron, 3/4-5/4-5/3 for the ratio of amorphous iron to organic carbon, and the 1/4-3/4-5/4 combination for organic carbon from the first site. These combinations of TM bands were selected by statistical correlation with soil chemical data.

The chemical data, DN values, and various band ratios were examined with the program package Statistix (NH Analytical Software) in order to find the combinations of reflectance data most likely to show a relationship which would dependably separate the exposed paleosols from other soils. Table 3 shows correlation coefficients (R) and P-values for the TM bands used individually. The best chance for success at predicting organic carbon levels and amorphous iron was with TM5 and TM7. There was no good relationship with free iron oxide. Apparently there was not enough difference expressed at the soil surface of the cultivated field to differentiate it by reflectance in these single wavebands.

Better results were obtained with band ratios (Table 4). Ratios having potential for discriminating organic carbon on this site were TM 1/4, 5/4, 5/7, 5/3, 5/2, 4/7, 3/5, 3/7, 4/1, and 4/5. The best candidates to discriminate amorphous iron were 5/4, 4/7, and 4/5. The analysis suggests only marginal success for free iron oxide with 3/4, 4/3, and 5/7. Since organic carbon and amorphous iron are inversely related, the ratio of the two is best modeled with the same bands indicated for organic carbon alone.

We also looked at combinations of three bands or three ratios to predict the soil properties (Table 5). The best relationships were for organic carbon and the ratio of amorphous iron to carbon followed by amorphous iron and free iron oxide in that order.

The TM band combination of 1/4-5/2-3/1 which was statistically correlated with organic carbon did not give a good result in the field. Patterns produced by the model were not understandable when compared to organic matter distribution in the field and the pattern of cluster distribution was not understood either. There was no recognizable soil line to guide our classification procedure and this model was

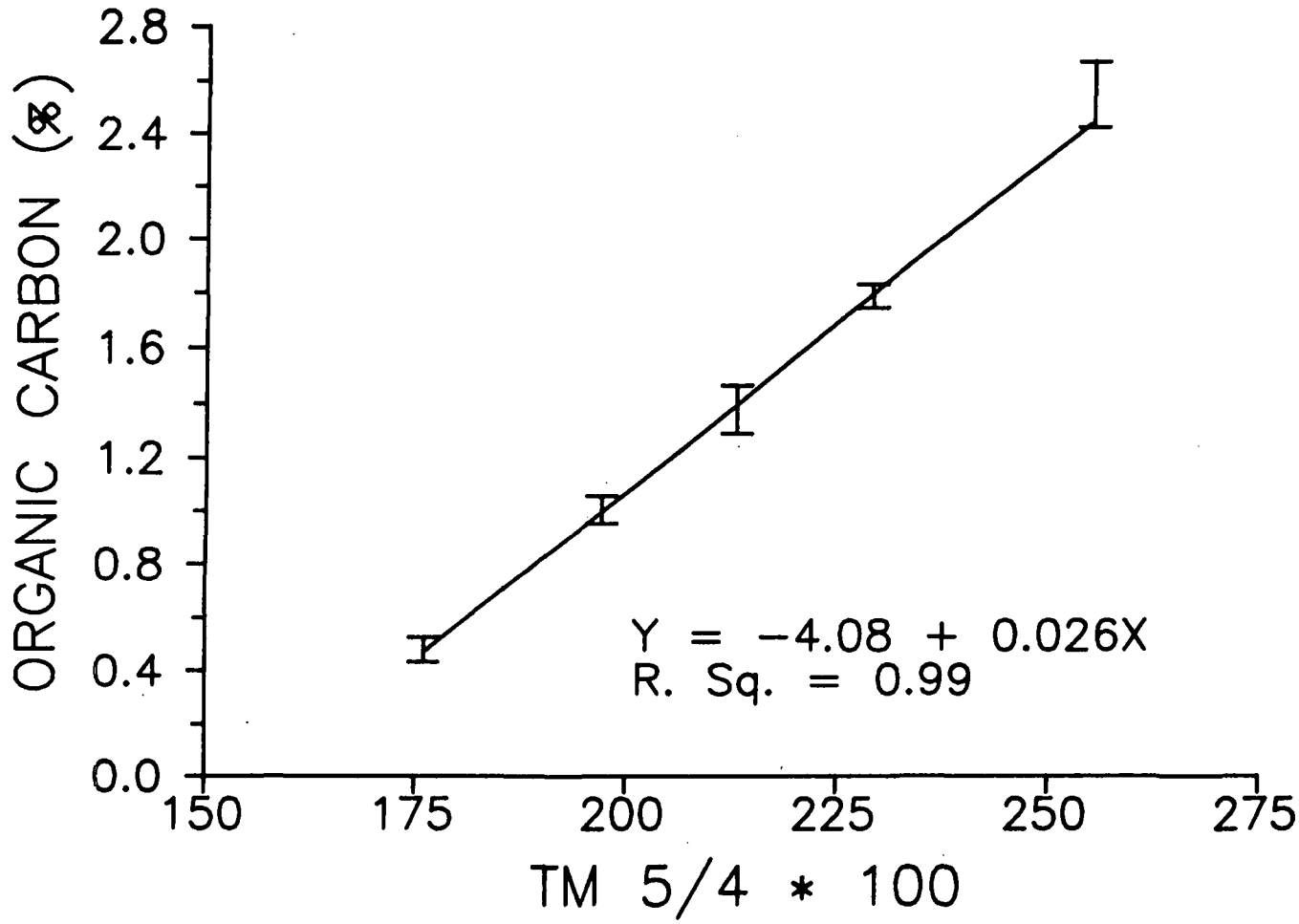

Figure 4. Regression line and equation for individual organic carbon samples and the mean DN of the TM 5/4 ratio. Error bars are standard error of the mean.

Table 3. Comparison of R and P values for reflectance and chemical data.

TM Band Ratio		Soil Properties			
		Organic Carbon	Amorphous Iron	Free Iron Oxide	Am Fe/OC
		g/Kg			
1 (Blue)	R	0.210	-0.271	-0.085	-0.286
	P	0.266	0.111	0.805	0.086
2 (Green)	R	-0.151	-0.085	-0.113	0.005
	P	0.504	0.805	0.684	0.999
3 (Red)	R	-0.194	-0.059	-0.160	0.064
	P	0.324	0.900	0.462	0.883
4 (IR1)	R	-0.257	0.011	-0.034	0.136
	P	0.138	0.996	0.966	0.573
5 (IR2)	R	0.398	-0.396	-0.072	-0.471
	P	0.008	0.009	0.856	0.001
7 (IR3)	R	0.538	-0.435	-0.172	-0.568
	P	0.000	0.003	0.411	0.000

Table 4. Comparison of R and P values for TM band ratios and chemical data.

TM Band Ratio		Soil Properties			
		Organic Carbon	Amorphous Iron	Free Iron Oxide	Am Fe/OC
		g/Kg			
1/4	R	0.557	-0.238	-0.032	-0.433
	P	0.000	0.182	0.969	0.003
3/4	R	0.094	-0.151	-0.323	-0.123
	P	0.768	0.506	0.043	0.637
5/4	R	0.703	-0.437	-0.046	-0.651
	P	0.000	0.003	0.939	0.000
5/7	R	-0.533	0.271	0.302	0.464
	P	0.000	0.110	0.064	0.001
5/3	R	0.538	-0.283	0.103	-0.742
	P	0.000	0.090	0.726	0.001
5/1	R	0.415	-0.366	-0.042	-0.463
	P	0.005	0.018	0.948	0.002
5/2	R	0.609	-0.372	0.034	-0.552
	P	0.000	0.015	0.966	0.000
3/1	R	-0.412	0.090	-0.184	0.278
	P	0.006	0.786	0.363	0.199
3/2	R	-0.211	0.005	-0.222	0.152
	P	0.264	0.999	0.229	0.498
4/7	R	-0.696	0.425	0.133	0.655
	P	0.000	0.004	0.589	0.000
3/5	R	-0.519	0.283	-0.085	0.464
	P	0.000	0.091	0.807	0.001
3/7	R	-0.611	0.333	0.011	0.550
	P	0.000	0.035	0.997	0.000

Table 4. Comparison of R and P values for TM band ratios and chemical data (continued).

TM Band Ratio		Soil Properties			
		Organic Carbon	Amorphous Iron	Free Iron Oxide	Am Fe/OC
		g/Kg			
4/1	R	-0.531	0.203	0.024	0.403
	P	0.000	0.292	0.982	0.007
4/2	R	-0.341	0.223	0.162	0.340
	P	0.030	0.224	0.456	0.031
4/3	R	-0.098	0.173	0.307	0.155
	P	0.749	0.405	0.058	0.489
4/5	R	-0.677	0.435	0.035	0.651
	P	0.000	0.003	0.964	0.000

Table 5. Selected combinations for mapping organic carbon, amorphous iron, free iron oxide, and ratio of Am Fe/OC.

Soil Properties	Combination (TM Bands)	R Square	P-value
Organic Carbon	1-4-7	0.562	0.000
	1/4-5/2-3/1	0.586	0.000
Amorphous Iron	3-4-5	0.300	0.011
	5/3-3/1-4/5	0.301	0.011
Free Iron Oxide	3-5-7	0.190	0.096
	5/3-3/5-4/7	0.193	0.092
Ratio of Am Fe/OC	3-4-5	0.517	0.000
	3/4-5/4-5/3	0.524	0.000

abandoned. The remaining three models were field tested by sampling within patterns produced by the models. Fifty-five soil samples were taken for all clusters. Chemical analyses for each sample included organic carbon (C) and amorphous iron (Fe_h). The means of organic carbon, amorphous iron, and the ratio of Fe_h/C were computed for the soil samples from each cluster location.

Amorphous iron model

TM band ratios 5/3, 3/1, and 4/5 were tested as a means to map the distribution of amorphous iron at the soil surface. Figure 5 shows a plot of the cluster distribution using TM 4/5 and 5/3. It shows a soil line made up of clusters 3, 4, 5, 8 and 10, and several other clusters which represent soils with partial cover by plants. In order to find the amorphous iron content of each cluster, the soils were sampled according to the classified image superimposed on a digitized topographic map. A colored version of this map is presented in Figure 6.

The results of the amorphous iron analyses are shown in Table 6. The iron content varies along the soil line from a low of 4.5 g/kg to 7.1 g/kg. Duncan's multiple range test says that there are only two different categories in this data, clusters 3 and 4 and clusters 5, 8 and 10 (Steel and Torrie, 1960). We have colored the classified image to show the patterns that we feel can be found in the field (Fig. 6). The color codes, chemical data, and DN values are presented in Table 7. The contour lines allow us to see that the highest levels of amorphous iron bearing soils are exposed along ridge tops and on convex slopes. To color the image to match the statistical output we would only need to combine red and yellow and add the pink areas to blue. This would show the most extreme exposure of the paleosols.

The amorphous iron contents of the surface soils sampled within each cluster were correlated with mean DN values for each cluster. The best relationship was with TM 5/3 (Fig. 7). Amorphous iron contents in g/kg can be predicted as 14.66 - 0.0537(TM 5/3 * 100) with R^2 of 0.98.

The reasons for seeing more patterns in the field and image than are shown by statistics are probably related to the interaction of amorphous iron and carbon. Covariance and correlation matrices computed for the soil sample data (Table 8) shows that organic carbon provided 87% of the variance and that there is a strong negative correlation between organic carbon and amorphous iron. The clusters are separated because of both factors; however, it is sure that clusters 3 and 4 represent the paleosols. They have amorphous iron contents typically found in these paleosols (Table 6).

Table 9 shows the distribution of amorphous iron in some typical profiles from the test field. The greatest amounts of amorphous iron are found in Bt horizons as compared to either C, BC, or A horizons. Some Ap horizons show higher values than A horizons because tillage

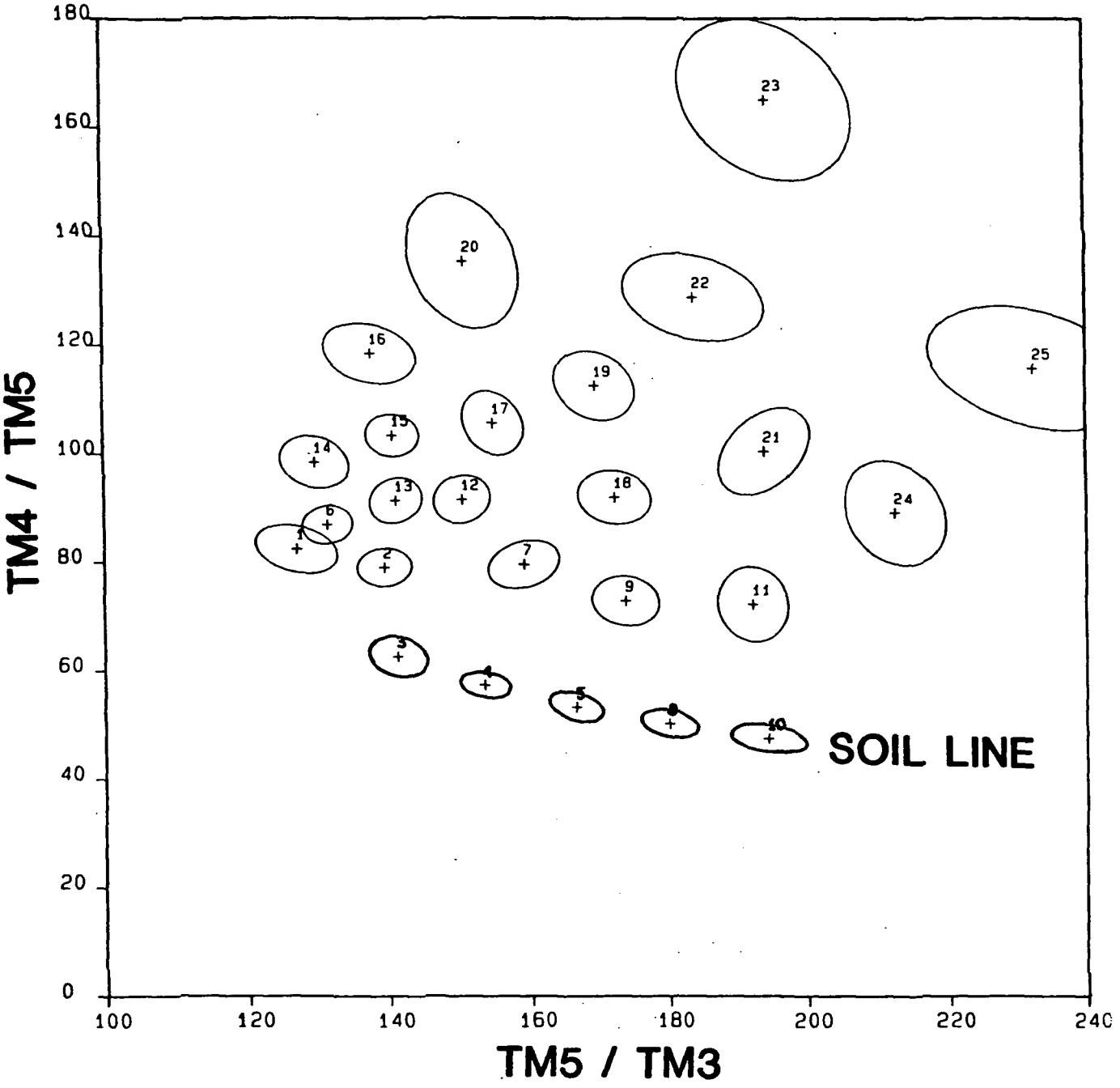

Figure 5. Cluster distribution of TM ratios 4/5, 5/3, 3/1, viewed from the 4/5, 5/3 side and showing a line of clusters from bare soil.

Table 6. Duncan's multiple range test for amorphous iron values.

Clusters	sample size	mean Fe_h	Duncan grouping
		(g/kg)	
3	15	7.1	A
4	15	6.5	A
5	8	5.1	B
8	5	4.5	B
10	9	4.6	B

Alpha = 0.05 DF = 33 MSE = 0.734

Number of means	2	3	4	5
Critical range	0.832	0.874	0.903	0.923

Means with the same letter are not significantly different

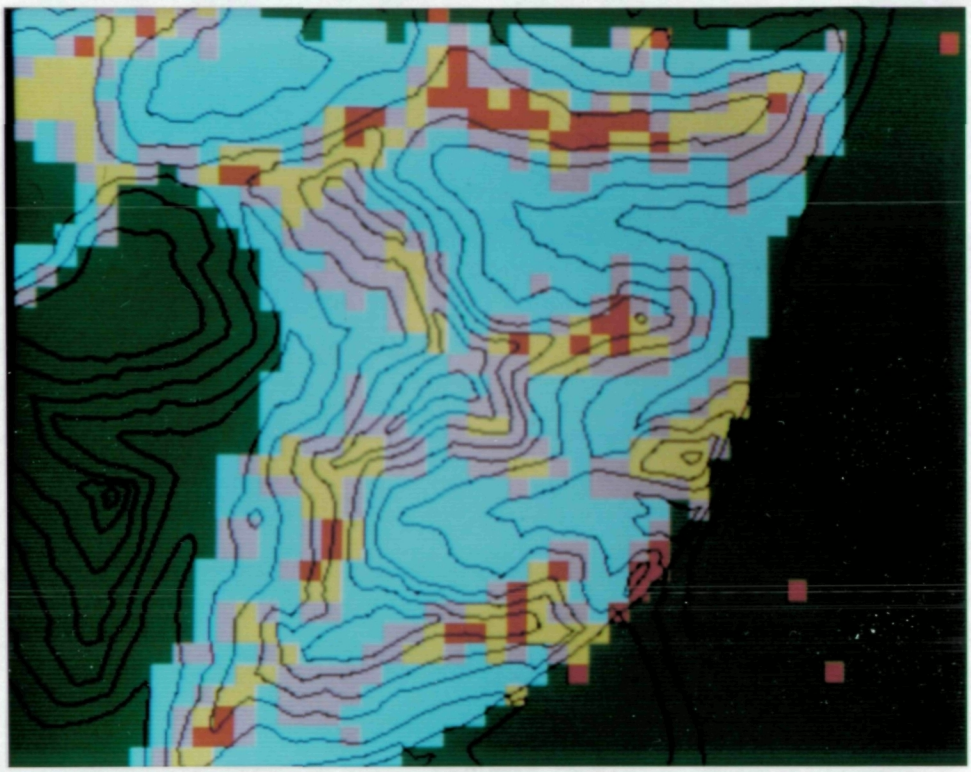

Figure 6. Model of amorphous iron mapped by TM ratios 5/3, 3/1 and 4/5 superimposed on 20 ft contour lines of a bare soil field. The content of iron in g/kg is red, 7.1; yellow, 6.5; pink, 5.5; and blue, 4.7. Plant cover is coded green.

Table 7. Characteristics of surface soils found within clusters of the amorphous iron model.

Cluster	Percent of scene	Mean DN value			Fe_h	Color coded
		TM5/3	TM3/1	TM4/5	(g/kg)	
3	5.70	141.4	72.5	62.6	7.10	Red
4	15.33	153.7	69.6	57.3	6.50	Yellow
5	23.14	166.6	67.1	53.4	5.10	Pink
8 & 10	55.83	187.3	63.1	48.9	4.60	Blue

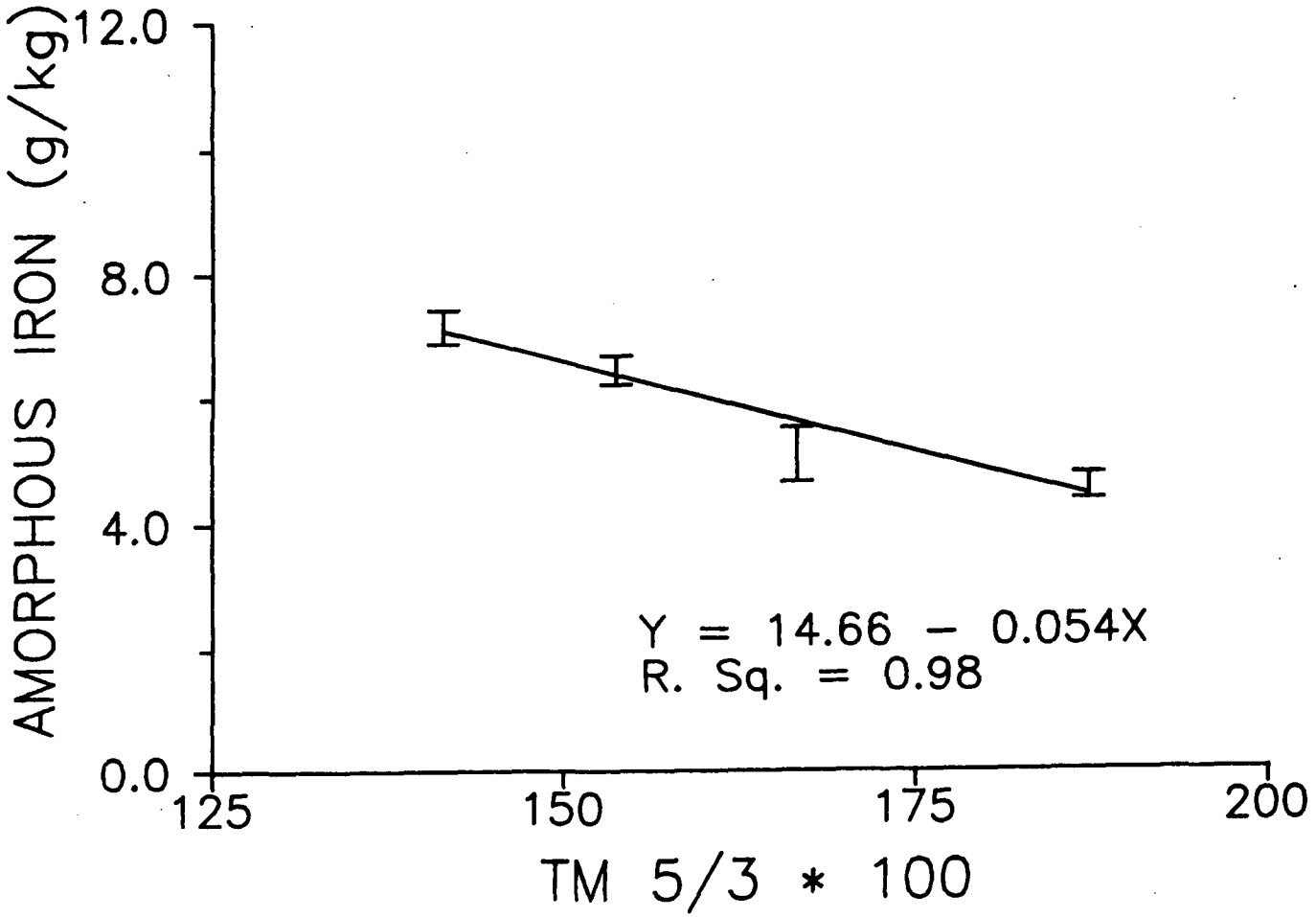

Figure 7. Regression line for amorphous iron with TM ratio 5/3.

Table 8. Variability and correlations of soil surface iron oxides and organic carbon.

Soil properties	C	Fe_h*	Fe_d**	Percent of variance
	Variance -- Covariance Matrix			
C	14.37			87.25
Fe_h	-2.817	1.119		6.79
Fe_d	-1.006	0.471	0.981	5.46
	Correlation Matrix			
C	1.000			
Fe_h	-0.7027	1.000		
Fe_d	-0.2681	0.4498	1.000	

*Fe_h = Fe extracted by hydroxylamine method, amorphous iron.
**Fe_d = Fe extracted by dithionite method, free iron oxide.

Table 9. Vertical distribution of iron oxides in soils from the test site.

Horizons	Depth (cm)	Amorphous iron	Free iron
		g/kg	
Thatuna series			
Ap	0-50	4.63	8.15
A	50-63	4.55	8.35
A/B	63-115	4.53	8.93
E	115-140	5.36	8.67
Btb	140-260	5.91	9.21
Naff series			
Ap	0-24	6.17	8.45
A	24-52	5.50	7.66
BA	52-77	6.03	6.18
Btb1	77-120	7.17	9.48
Btb2	120-210	7.18	8.64
Palouse series			
A	0-35	4.29	9.55
B/E	35-40	5.57	9.60
Btb	40-100	7.44	10.81
BC	100-135	5.81	10.74
Garfield series			
Ap	0-13	5.69	9.44
Btb	13-33	8.46	10.57
C	33-87	5.14	10.50

overburden contains B material that has been moved down slope.

Organic Carbon Model

The carbon model is the same as that reported for the first site. The soil line parallels the Y axis (TM 5/4) of the cluster plot. Table 10 shows the organic carbon contents found at the soil surface in each of the clusters of the soil line. It ranges from 5 g/kg to 21 g/kg. The statistical analysis again shows that not all clusters are different. In some cases this is probably related to the small sample size. We sampled only those clusters where we were sure of our location.

A color coded map of the organic carbon model is shown in Figure 8. It is colored in one of several possible ways following the results of Duncan's multiple range test. The color code and cluster combinations are shown in Table 11 along with the DN values. The classes are well separated, having about 4 g/kg difference in carbon between them. This result corroborates our findings with this model on the first site.

Figure 9 shows the linear regression of mean organic carbon values with mean TM 5/4 DN values. The content of organic carbon in g/kg can be predicted by the equation $-43.4 + 0.297(\text{TM } 5/4 * 100)$ with an R^2 of 0.98. In our earlier test we computed an equation for organic carbon in percent, $-4.08 + 0.026$ (TM 5/4 * 100) with an R^2 of 0.99. (This second equation can be made equivalent to the first equation by multiplying the coefficients by a factor of 10.) The differences between these two equations are small. The difference in prediction of organic carbon is about 0.5%. Differences may be caused by the fact that data are taken from two widely separated areas and from images of two different years. No attempts have been made to correct the image data for these differences.

Fe_h/C ratio model

The ratio of Fe_h/C was being investigated because of reports in the literature which relate a decrease in the ratio to increased effects of erosion (Pazar, 1983), and because we have noticed that the organic carbon model and the amorphous iron model used separately each found a few eroded areas not distinguished by the other. Since amorphous iron and organic carbon are inversely related they have the potential of showing good results if used together.

The best spectral combination for this model was TM 3/4, 5/4, and 5/3. Figure 10 shows the cluster distribution for the model. The soil line is parallel to the TM 5/3 axis. Table 12 shows the Fe_h/C ratios found in the field data for those clusters and gives the Duncan multiple range test grouping for the data. Again, it is probable that small sample size keeps the test from showing separations that we think can be made in the field.

By regressing these ratio values on the corresponding DN values of

Table 10. Duncan's multiple range test for organic carbon.

Clusters	sample size	mean C (g/kg)	Duncan grouping	
27	7	21.08		A
26	5	16.01		B
24	4	13.43	C	B
25	3	11.87	C	D
23	6	10.06	E	D
22	12	8.28	E	
21	13	5.04		F

Alpha = 0.05 DF = 31 MSE = 5.710

Number of means	2	3	4	5	6	7
Critical range	2.915	3.063	3.165	3.230	3.283	3.325

Means with the same letter are not significantly different

ORIGINAL PAGE
COLOR PHOTOGRAPH

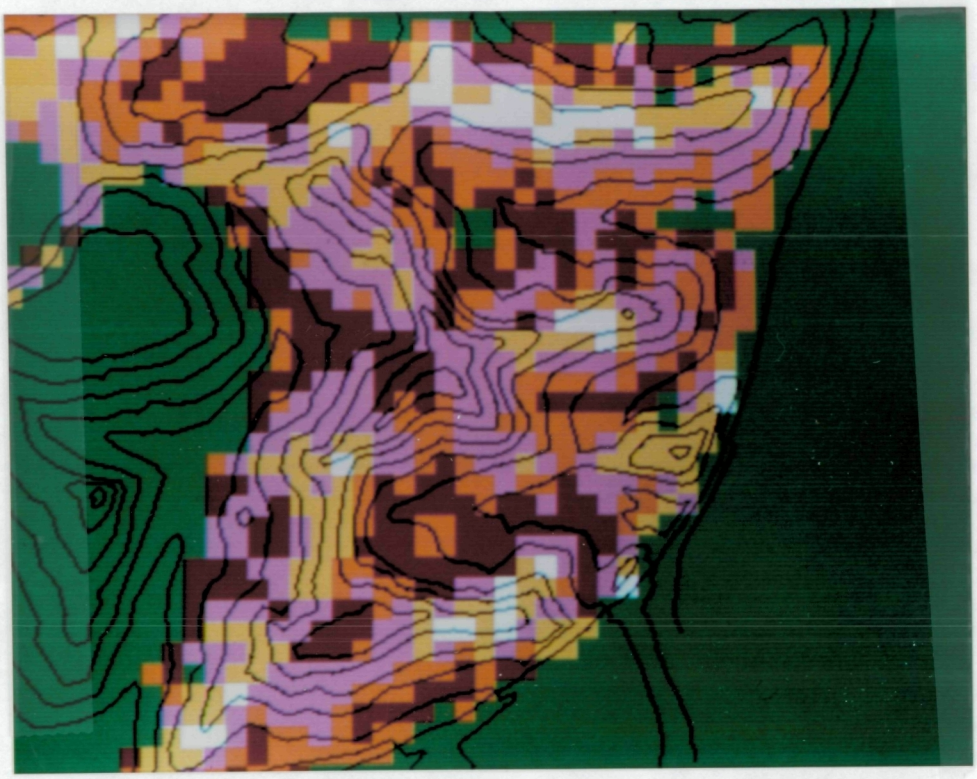

Figure 8. Model of organic carbon mapped by TM ratios 1/4, 3/4 and 5/4 superimposed on 20 ft contour lines of a bare soil field. The content of organic carbon in g/kg is white, 5.0; yellow, 9.0; pink, 12.2; orange, 16.0; and dark red, 21.0. Plant cover is coded green.

Table 11. Characteristics of surface soil found within clusters of the organic carbon model.

Cluster	Percent of scene	Mean DN value			C	Color coded
		TM1/4	TM3/4	TM5/4	(g/kg)	
27	26.37	180.7	112.4	213.6	21.10	Dark red
26	22.60	169.6	110.2	201.8	16.00	Orange
24 & 25	29.23	170.6	113.6	190.5	12.70	Pink
22 & 23	17.62	165.6	113.4	174.9	9.20	Yellow
21	4.18	157.5	114.3	161.9	5.00	White

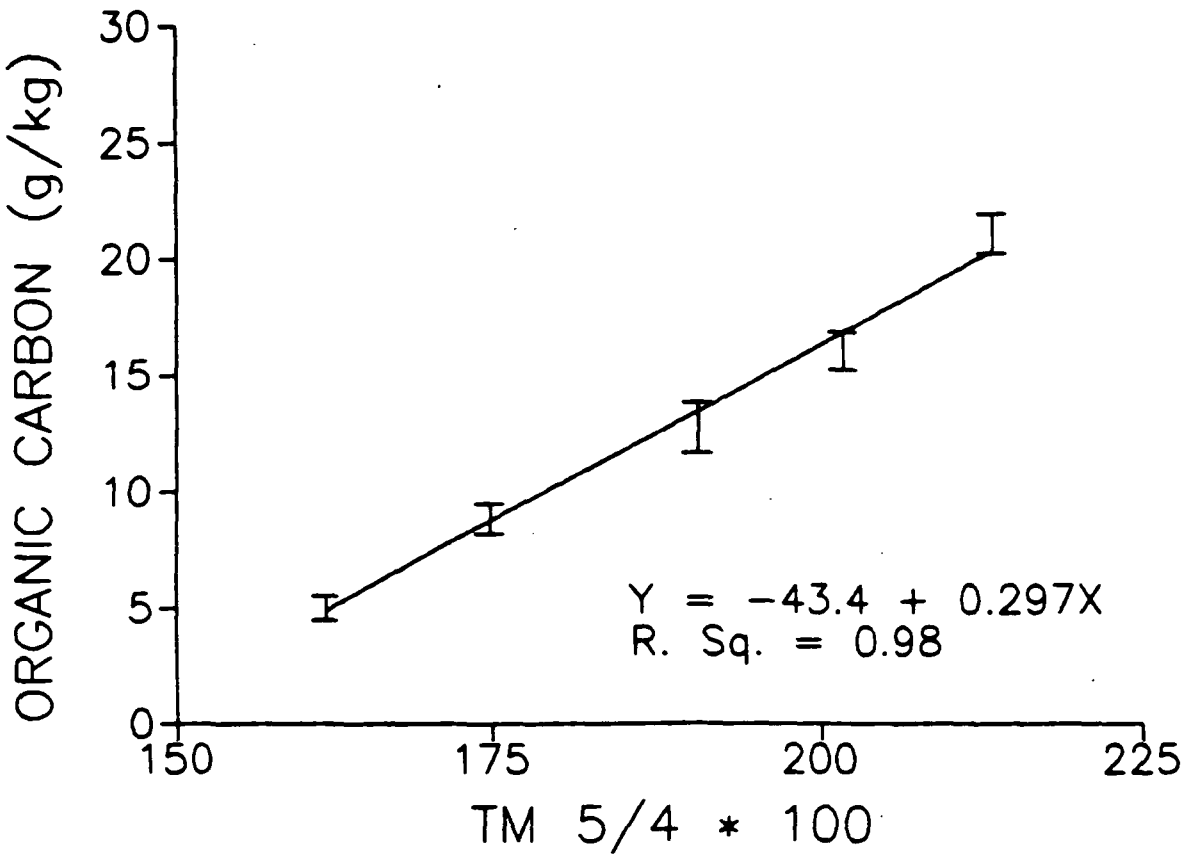

Figure 9. Regression line for organic carbon with TM ratio 5/4.

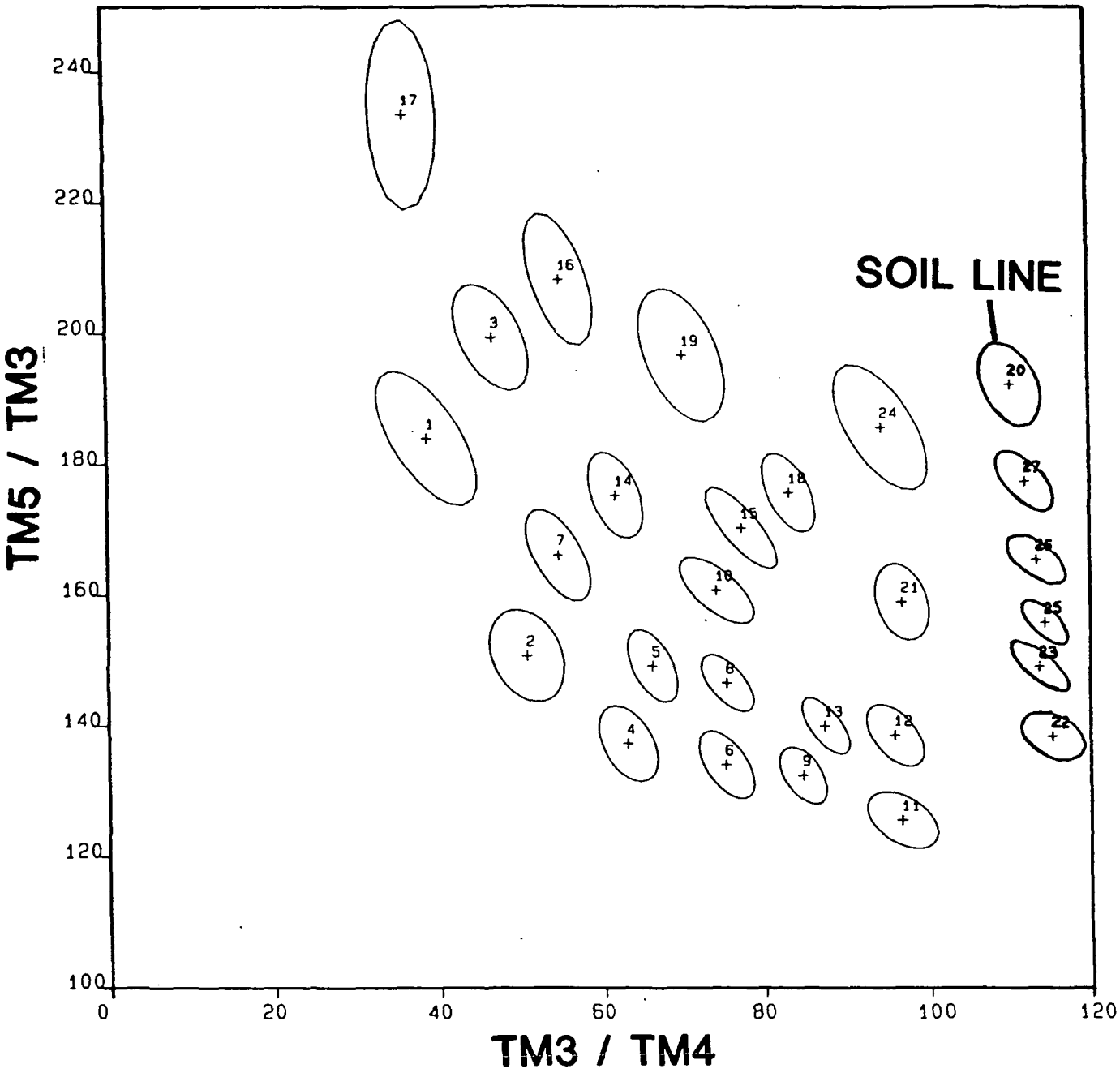

Figure 10. Cluster distribution of TM ratios 3/4, 5/4, 5/3 viewed from the 5/3, 3/4 side. The soil line clusters are oriented according to the Fe_2O_3/C ratio, with the least amount of carbon represented be the lowest cluster in the line.

TM 5/3, the ratio of Fe_b/C is found to be a power function of TM 5/3. There is a significant correlation between them (R^2 = 0.96). The function is $Fe_b/C = 1.437 * 10^{16} * (TM\ 5/3 * 100)^{-6.516}$ (Fig. 11). This function is useful because it allows maximum separations to be made in the eroded soils, which are at the steep end of the curve. Table 13 shows the color codes, Fe_b/C ratios and DN values for the model as presented in Figure 12. No clusters have been combined, though according to the statistical tests, some could be. It is our impression after having been in the field with this model that the effects of erosion are shown very well.

It is useful to compare the results of these three models. Table 14 shows selected data from each model and the amount of area classified by each cluster. The organic carbon and amorphous iron models are virtually identical with respect to the amount of iron found in the clusters. The carbon model has one additional class at the high end and could conceivably have more classes if used on fields with more carbon. The model for Fe_b/C makes a different division of the spectral values at the low carbon end of the soil line. Cluster 22 shows soils that have suffered the severest erosion. There is no hint of any soil horizon which may have contained carbon remaining on them. The soils in clusters 23 and 24 are only slightly better.

Site Three

Composite Spectra

Composite spectra were investigated at a third site where partly vegetated clusters could be reliably located in the field using aerial photography. The sampling problem was compounded because the imagery was two years old at the time of sampling; however, the aerial photography was useful to locate patches of green cover which corresponded to data clusters from the TM imagery. In this manner, it was possible to sample the soils in some of the clusters which did not fall on the soil line. It was not possible to sample the density of plant cover; however, it may be expected for reasons described earlier that clusters positioned closer to the origin of the plot have more plant cover than those near the soil line (Figure 13).

Results of organic carbon analyses showed that clusters not on the soil line are distributed parallel to the soil line because of variation in the amount of organic carbon. In Figure 13, sampled clusters are labeled with carbon values or a range of values. It is evident that clusters of composite spectra along the lower side of the triangle have low carbon values and clusters along the upper side have higher values. And it appears that if carbon values from soil line clusters are known then it is possible to predict the carbon values of soils with composite spectra by projecting lines of similar carbon value from the soil line to the point of greenness.

Two such lines are shown for 0.4% and 1.0% organic carbon. As the lines converge toward the point of greenness the soil contribution to the composite spectra is reduced. According to Huete et al. (1985)

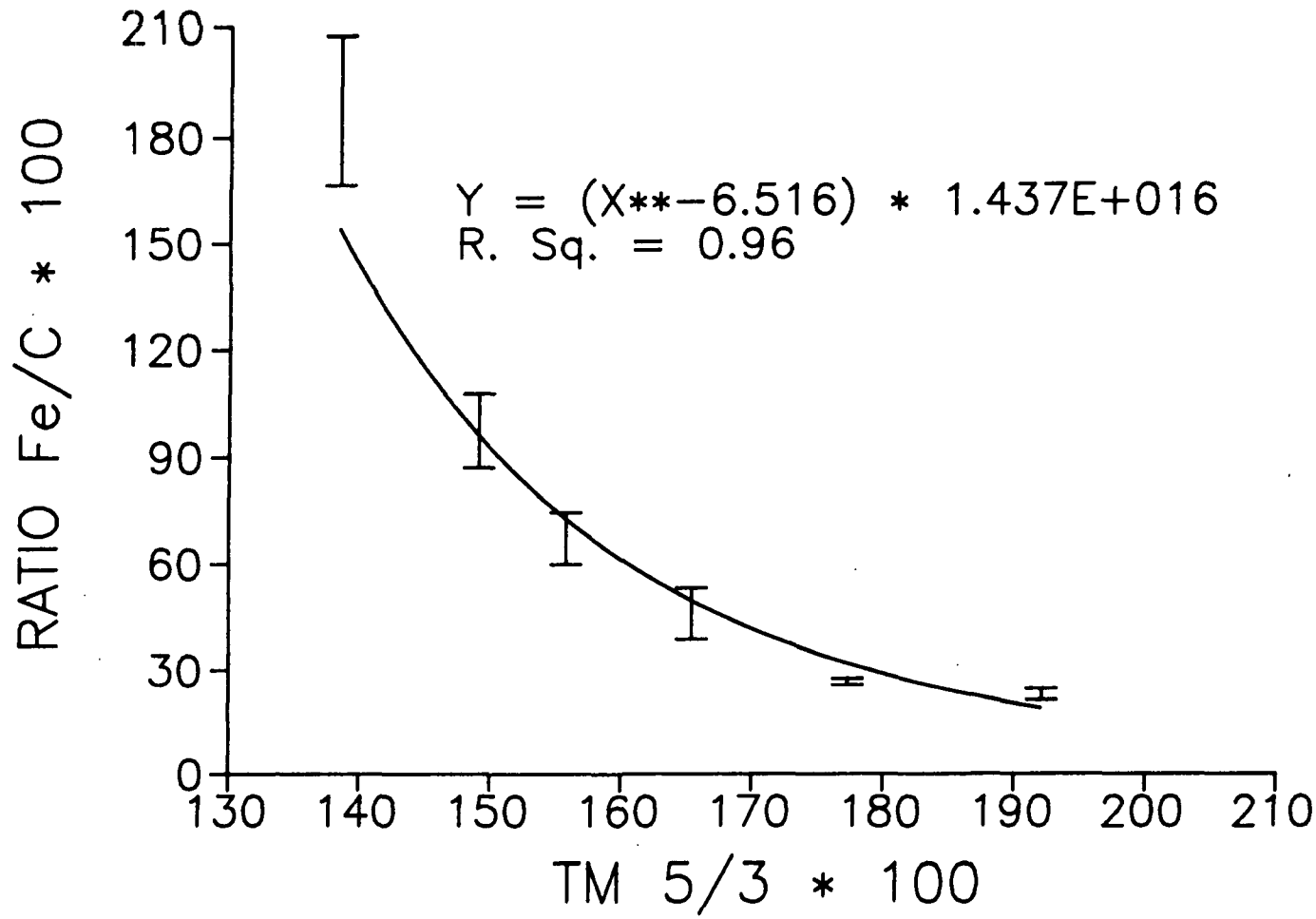

Figure 11. Regression line for the Fe_h/C ratio with TM ratio 5/3.

Table 13. Characteristics of surface soil found within clusters of the Fe_h/C model

Cluster	Percent of scene	Mean DN value			Fe_h/C (*100)	Color coded
		TM3/4	TM5/4	TM5/3		
20	30.27	110.4	212.1	192.1	23.50	Dark red
27	33.20	112.1	198.7	177.3	26.80	Red
26	16.00	113.5	187.7	165.4	46.00	Pink
25	10.03	114.5	178.3	155.8	67.00	Light pink
23	7.57	113.8	169.6	149.1	97.40	Yellow
22	2.93	115.4	159.5	138.4	187.10	White

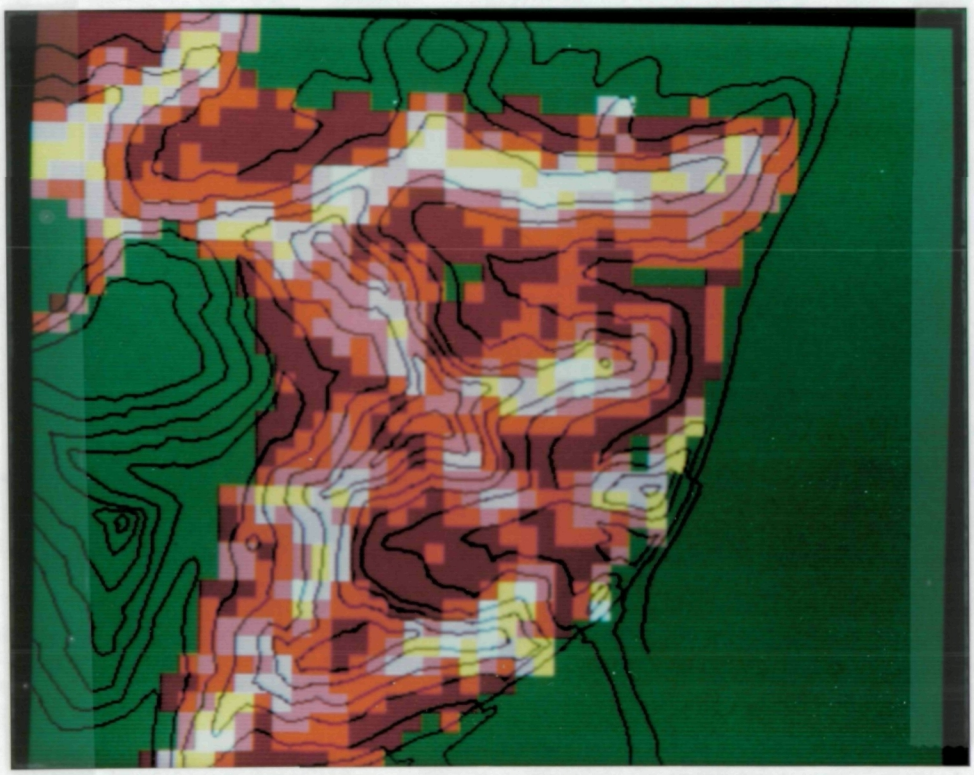

Figure 12. Model of the Fe_h/C ratio mapped by TM ratios 3/4, 5/4 and 5/3 superimposed on 20 ft contour lines of a bare soil field. The ratio * 100 is white, 187.1; yellow, 97.4; light pink, 67.0; pink, 46.0; red, 26.8; and dark red, 23.5. Plant cover is coded green.

Table 14. Comparison of three models.

Cluster	Fe_h ------g/kg------	C	Fe_h/C ------ *100	Percent of scene
		Model for Amorphous iron		
3	7.1	4.9		5.7
4	6.5	8.6		15.3
5	5.1	12.3		23.2
8 & 10	4.6	17.2		55.8
		Model for organic carbon		
21	7.1	5.0		4.2
22 & 23	6.3	9.2		17.6
24 & 25	5.0	12.7		29.2
26	4.6	16.0		22.6
27	4.5	21.1		26.4
		Model for Fe_h/C		
22	7.4	4.0	187.1	2.9
23	6.8	7.0	97.4	7.6
25	6.2	9.3	67.0	10.0
26	5.3	11.5	46.0	16.0
27	4.0	14.9	26.8	33.2
20	4.6	19.6	23.5	30.3

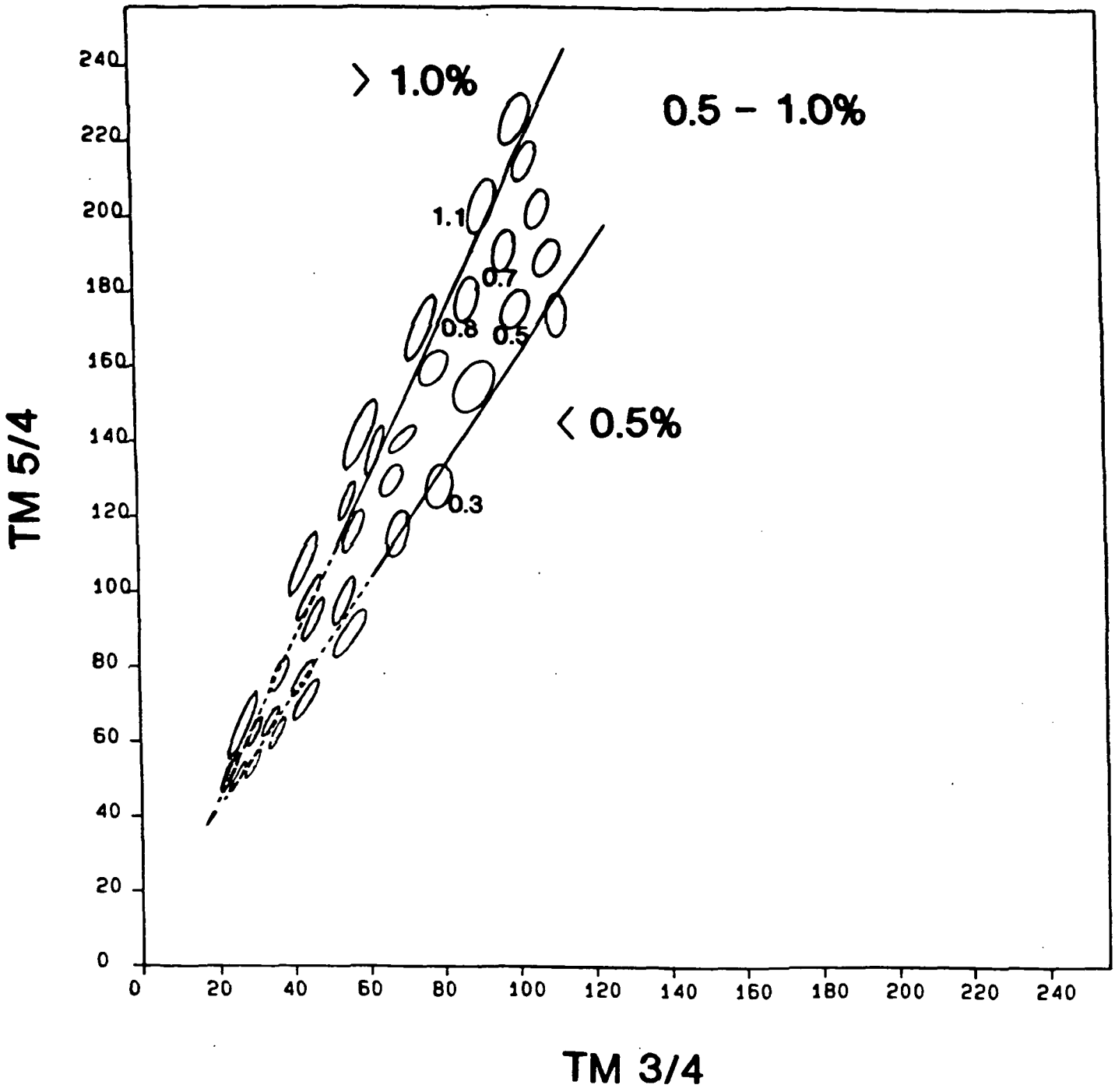

Figure 13. Organic carbon content (%) of TM ratio data clusters which are offset from the soil line because of a green plant reflectance component. Two lines form sides of a conceptual triangle, beginning at the point of greenness, the lower side is drawn at 0.4% carbon and the upper side at 1.0% carbon.

there should be little influence of soil on the composite spectra after plant cover exceeds 90%. It is not known exactly where this point is in Figure 13 since plant cover was not measured; consequently the lines predicting soil organic carbon have been left dotted in the untested area.

II. Using selected test sites, estimate the extent of eroded agricultural soils of the Palouse region and establish baseline information for comparison with future estimates.

Using the carbon class map from the first test site and our knowledge of the soils derived from field sampling we found 1039 ha (2569 ac) of bare soil (Table 15). Paleosols which have been completely exposed by erosion occupy 2.7% of the area. Low carbon areas on steep south-facing slopes with soils 1 m (3.3 ft) or less in depth occupy 20% of the area. These have about 16 cm (6.3 in.) of epipedon remaining. The moderate carbon class covers 44% of the area, has soils with 30 cm (11.8 in.) epipedons, and has about 1.3 m (4.3 ft) of soil over a lime-silica paleosol. The high carbon area covers 28.8% of the site, has soils with 36 cm (14.2 in) to 46 cm (18.1 in) epipedons and averages 1.3 m (4.3 ft) to a paleosol. Low-lying areas with the highest carbon content are 4.4% of the area. This class should show much more area, but most of it has been covered with alluvial soil from upper slope positions and is accurately mapped (according to organic carbon content) into several of the other carbon classes.

Approximately 20% of the second test site suffers from substantial erosion, enough to expose the paleosols. And on the other end of the scale, about 63% has accumulated sediment or has only slight erosion. The remaining 17% is on sloping land (pink areas shown in Fig. 6) and is highly susceptible to erosion.

III.

Aerial photographs taken in 1939 were obtained of two study sites; however, these proved to be very difficult to analyze. It was a matter of guesswork to determine which areas were in summer fallow and which were covered with stubble. There was much uncertainty about the appearance of exposed paleosols under these conditions. We finally decided that the old black and white photos would not yield useful and comparable data so this objective was abandoned to prevent the reporting of unreliable data.

CONCLUSIONS

It is concluded from this study that TM data may be effectively used in the form of band ratios to distinguish levels of organic carbon in soils that are dry, do not have greater than about 1% iron oxide, have uniform particle size (mostly siltloams) and that are not covered with plant residue. Plotting the ratios TM 5/4 against 3/4 allows one to see the relationships of the soils to each other and to the green plant material. Plotting TM 5/4 against 1/4 is useful to see the distribution of the soil line data clusters as a plane.

Table 15. Area of exposed paleosols and organic carbon levels.

	Carbon percent	Area		
		Percent	Acres	Hectares
Bk Paloesols	0.43	0.7	18	7
Bw Paleosols	0.53	2.0	52	21
Steep South Slopes	1.00	20.0	514	208
Moderate South Slopes	1.38	44.0	1131	458
Summits and North Slopes	1.78	28.8	740	299
Flat, Low-Lying	2.55	4.4	114	46
TOTAL			2569	1039

Organic carbon is the main factor influencing the distribution of data clusters along the soil line which is found by plotting TM 5/4 and 3/4. Organic carbon may be modeled by $Y = -3.91 + 0.025(TM\ 5/4 * 100)$, $R^2 = 0.81$. Where the carbon content was less than 1%, separate clusters were mapped for soils with iron enriched horizons and lime-silica enriched horizons exposed at the surface.

The organic carbon content may be estimated for soils that are partly covered with green vegetation if a TM 5/4, 3/4 cluster plot is available and it has a point of greenness and a bare soil line. The organic carbon content must be known for the soil line. Then the carbon content of clusters which are offset from the soil line because of green vegetation may be estimated because their brightness in TM 5/4 remains the same relative to their organic carbon content.

For Palouse region soils, it appears that the ratio of Fe_h/C is useful to define the effects of erosion on the exposure of the paleosols. The Fe_h/C ratio may be modeled by a power function of TM 5/3. The $Fe_h/C = 1.437 * 10^{16} * (TM5/3 * 100)^{-6.516}$.

Based on the test fields we have used, on the order of 20% of Palouse region soils are made up of paleosols at or near the surface. This is a result of erosion removing more recent and desirable soils.

LITERATURE CITED

Crist, E. P., and R. C. Cicone, 1984. A physically-based transformation of Thematic Mapper data - The TM tasseled cap. IEEE Trans. Geosci. Remote Sens. GE-22(3):256-263.

Frazier, B. E., and A. J. Busacca, 1987. Satellite assessment of erosion. In L. F. Elliott (ed), STEEP-Conservation Concepts and Accomplishments, Washington State University Press, Pullman, WA pp. 579-584.

Hart, J. A., and D. B. Wherry, (eds), 1984. VICAR/IBIS user reference manual. Graphics and Image Analysis Group, Computing Service Center, Washington State University, Pullman, WA

Huete, A. R., R. D. Jackson, and D. F. Post, 1985. Spectral response of a plant canopy with different soil backgrounds. Remote Sens. Environ. 17:37- 53.

Jensen, J. R., 1986. Introductory digital image processing - A remote sensing perspective. Prentice-Hall, Englewood Cliffs, NJ

Kanemasu, E. T., 1974. Seasonal canopy reflectance patterns of wheat, sorghum, and soybeans. Remote Sens. Environ. 3:43-47.

Kauth, R. J., and G. S. Thomas, 1976. The tasseled cap - a graphic description of the spectral-temporal development of agricultural crops as seen by Landsat. Proc. Symp. Machine Process. Remote Sens. Data, Purdue Univ., West Lafayette, IN, pp. 4B41-4B51.

Kauth, R. J., P. F. Lambeck, W. Richardson, B. S. Thomas, and A. P. Pentland, 1979. Feature extraction applied to agricultural crops as seen by Landsat. In The LACIE Symp, Proc. Tech. Sessions, NASA Johnson Space Center, vol 2:705-721.

Kittrick, J. A., and E. W. Hope. 1963. A procedure for the particle-size separation of soils for X-ray diffraction analysis. Soil Sci. 96:319-325.

Kriegler, F. J., W. A. Malila, R. F. Nalepka, and W. Richardson, 1969. Preprocessing transformations and their effects on multispectral recognition. In Proc. Sixth International Symp. Remote Sens. Environ. Vol 1:97-117.

Nelson, D. W., and L. E. Sommers, 1975. A rapid and accurate procedure for estimation of organic carbon in soils. Indiana Acad. of Sci. Proc. 84:456- 462.

NH Analytical Software, 801 West Iowa Avenue, St. Paul MN 55117

Pazar, S. E. 1983. Spectral characteristics of iron oxide and organic matter in eroded soils. Unpublished M.S. Thesis, Purdue Univ., West Lafayette, IN

Ross, G. J., C. Wang, and P. A. Schuppli, 1985. Hydroxylamine and ammonium oxalate solutions as extractants for iron and aluminum from soils. Soil Sci. Soc. Am. J. 49:783-785.

Schollenberger, C. J., 1927. A rapid approximation method for determining soil organic matter. Soil Sci. 24:65-68.

Steel, R. G. D., and J. H. Torrie. 1960. Principles and procedures of statistics. McGraw-Hill Book Company, Inc., New York, NY

U. S. Department of Agriculture, 1984. Procedures for collecting soil samples and methods of analysis for soil survey. Soil Cons. Serv., Soil Surv. Invest. Rep. No. 1.